Chemical Science

ROYAL SOCIETY OF CHEMISTRY

EDGE ARTICLE

View Article Online
View Journal

Cite this: DOI: 10.1039/d6sc01780k

All publication charges for this article have been paid for by the Royal Society of Chemistry

Slow cooling and efficient extraction of hot carriers in perovskite films *via* engineering trap-mediated relaxation channels

Xinlei Zhang,[ab] Jing Leng,[*b] Qi Sun,[b] Qingshun Dong,[b] Xinyu Tong,[b] Yu Song,[a] Yan Xu,[*a] Shengye Jin[*b] and Wenming Tian[*b]

Received 3rd March 2026
Accepted 28th April 2026

DOI: 10.1039/d6sc01780k

rsc.li/chemical-science

Long-lived hot carriers (HCs) are highly desired for HC photovoltaics, but achieving slow HC relaxation is challenging because strong electron-phonon interaction typically drives rapid thermalization. Herein, we investigate the influence of excess PbI_2 on HC relaxation in formamidinium lead iodide ($FAPbI_3$) perovskite films using femtosecond transient absorption spectroscopy. Our results show that excess PbI_2 significantly slows down the HC relaxation at high excitation densities, extending their lifetime to hundreds of picoseconds. This effect arises from intraband trap states (ITSs) introduced by excess PbI_2, enabling an ITS-mediated channel that suppresses direct HC relaxation under high densities due to a hot phonon bottleneck. Owing to the remarkably suppressed HC relaxation, efficient HC extraction was successfully achieved in PbI_2-rich perovskite films by incorporating electron acceptors. Our findings suggest an effective approach to prolong the HC lifetime in perovskite films *via* engineering ITSs, offering valuable guidance for the rational design of high-efficiency HC photovoltaic devices.

Introduction

Due to the presence of the Shockley–Queisser (S–Q) limit, the power conversion efficiency (PCE) of single-junction solar cells is fundamentally constrained.[1–3] This limitation primarily results from the rapid dissipation of excess energy in the form of heat during carrier thermalization. To overcome this limit, the concept of hot-carrier solar cells has been proposed, aiming to extract hot carriers (HCs) before thermalization and achieve efficiencies beyond the S–Q limit.[4,5] Recently, lead halide perovskites have emerged as a promising candidate for solar energy conversion owing to their strong and broad absorption, large diffusion coefficient, long carrier lifetimes, and tunable bandgaps.[6–11] In particular, under high excitation densities, this class of materials exhibit a significant hot phonon bottleneck (HPB) effect due to their large electron-phonon interaction, which greatly slows down the HC relaxation process and thereby extends their lifetime to tens of ps.[12–15] This feature enables perovskite materials to show great potential for efficient HC extraction, offering a new opportunity to break the S–Q limit for high-efficiency photovoltaic applications.

Recently, it has been discovered that incorporating polar cations into perovskite films can introduce new intraband intermediate states, thereby significantly slowing down the HC relaxation process *via* altering their relaxation pathway, which provides another effective way to extend the lifetime of HCs.[16] As is well known, for perovskite solar cells with relatively high efficiency (≥20%), excess PbI_2 is often found to aggregate at the grain boundaries and interfaces of perovskite films, indicating that residual PbI_2 might play an important role in affecting their carrier dynamics and device performance.[17–19] A lot of experimental studies have confirmed that an appropriate excess of PbI_2 can passivate grain-boundary defects, improve crystallinity, and enhance device performance;[20,21] however, excessive PbI_2 may also lead to the increase of nonradiative recombination centres and the reduction of photovoltaic efficiency.[22–24] Meanwhile, some theoretical studies have also shown that excess PbI_2 may easily lead to the formation of some defects, such as iodine vacancies and interstitial iodine, due to their low formation energies.[25,26] These defect levels are even found to be likely higher than the conduction band minimum (CBM) or valence band maximum (VBM),[27] suggesting that excess PbI_2 might affect the lifetime of HCs by modifying their relaxation pathway. Although the impact of excess PbI_2 on defect formation and band-edge carrier kinetics in perovskite films, as well as their device performances, has been widely reported,[28–30] it is still unclear how it influences the HC relaxation dynamics.

Formamidinium perovskite ($FAPbI_3$) has garnered broad attention due to its narrower bandgap and better stability.[31–34] Herein, we take $FAPbI_3$ films as an example to investigate the influence of excess PbI_2 on their HC relaxation by using femtosecond transient absorption (TA) spectroscopy. The

[a]Department of Chemistry, College of Sciences, Northeastern University, Shenyang 110819, China. E-mail: xuyan@mail.neu.edu.cn

[b]State Key Laboratory of Chemical Reaction Dynamics, Dalian Institute of Chemical Physics, Chinese Academy of Sciences, Dalian 116023, China. E-mail: ljjx@dicp.ac.cn; sjin@dicp.ac.cn; tianwm@dicp.ac.cn

results show that under high excitation intensities, the relaxation process of HCs in $FAPbI_3$ films with excess PbI_2 can be greatly slowed down, leading to their lifetime of up to hundreds of ps. It is because excess PbI_2 can introduce new intraband trap states (ITSs), thereby enabling an ITS-mediated HC relaxation pathway at high excitation densities, which, however, is absent at low excitation densities. This discrepancy is mainly a result of the competition between the direct and ITS-mediated relaxation channels of HCs under different densities. By incorporating appropriate acceptors, we successfully achieved the efficient extraction of HCs in $FAPbI_3$ films containing excess PbI_2 due to the prolonged HC lifetime. Our findings demonstrate a practical way to suppress HC relaxation in perovskite films *via* precise control of PbI_2 content, which might be of great significance for improving the performance of HC photovoltaic devices.

Results and discussion

In this work, in order to study the effect of excess PbI_2 on carrier dynamics in perovskite films, we prepared five batches of $FAPbI_3$ films with different PbI_2 contents using a previously reported two-step method,[35] in which the PbI_2 content was controlled by adjusting the PbI_2 concentration in their precursors (more details about material preparation can be found in the SI). For convenience, these as-prepared perovskite films are denoted as $FAPbI_3$-*x*, where *x* represents the PbI_2 concentration in their precursors (*i.e.*, $FAPbI_3$-1 M, $FAPbI_3$-1.25 M, $FAPbI_3$-1.5 M, $FAPbI_3$-1.75 M and $FAPbI_3$-2 M). The representative SEM images of these samples are presented in Fig. S1, showing pronounced segregation along grain boundaries. As shown in Fig. 1a and S2, the UV-vis absorption spectra of these samples exhibit the same characteristic peaks at ~785 nm, while the peak positions of their photoluminescence (PL) spectra are located at ~803 nm, both consistent with previous reports.[36] The crystal structure and crystallinity of these films were further examined by X-ray diffraction (XRD). As shown in Fig. 1b, all as-prepared $FAPbI_3$ films display diffraction peaks at 14° and 28.1°, corresponding to the (100) and (200) planes of α-phase $FAPbI_3$, respectively.[37,38] With the increase of PbI_2 content, another diffraction peak at 12.5° (corresponding to the (001) plane of PbI_2) begins to appear from PbI_2 concentration >1.5 M, and its intensity gradually increases.[39] These observations strongly confirm the coexistence of perovskite and PbI_2 phases in these films and also demonstrate that PbI_2 contents in the films can be effectively tuned by controlling the PbI_2 concentration in the precursors.

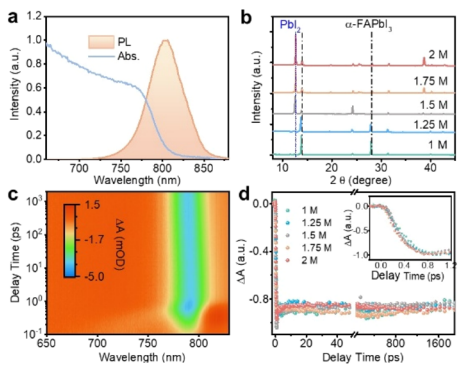

Fig. 1 Optical properties of $FAPbI_3$ films with different PbI_2 contents. (a) UV-vis absorption and PL spectra of $FAPbI_3$-1.5 M. (b) XRD patterns of $FAPbI_3$ films with different PbI_2 contents. (c) 2D pseudo-color image of TA spectra of $FAPbI_3$-1.5 M under 400 nm excitation at a low fluence of 0.1 μJ cm^{-2}. (d) Comparison of XB kinetics of five kinds of $FAPbI_3$ films under 400 nm excitation at a fluence of 0.1 μJ cm^{-2}.

We first investigated the carrier dynamics in these samples under low excitation intensities by using femtosecond TA spectroscopy (see the SI for more details). Fig. 1c presents the representative two-dimensional (2D) pseudo-color TA maps of $FAPbI_3$-1.5 M sample under 400 nm excitation with a low fluence of 0.1 μJ cm^{-2}, and its corresponding TA spectra at different delays are shown in Fig. S3. The TA spectra exhibit a pronounced exciton bleaching (XB) peak centered at 793 nm,[40] consistent with its steady-state absorption spectrum (Fig. 1a). The XB signal originates from the state filling of band-edge carriers, and thus its kinetics exactly represents the time evolution of band-edge carriers after photoexcitation.[41] Fig. S4 plots the 2D pseudo-color TA images of other samples with different PbI_2 contents, and their corresponding XB kinetics are also compared in Fig. 1d, showing similar spectral features and kinetic behavior. These similar spectra, as well as their similar XRD patterns, between various samples indicate that excess PbI_2 hardly alters the bandgap and crystal structure of perovskite films. We note that the XB kinetics in all samples exhibit ultrafast rise (<1 ps) (see the inset of Fig. 1d), indicating that their HCs undergo rapid relaxation to the band edge under low excitation intensities.

To study the effect of excess PbI_2 on HC relaxation, we next performed TA measurements on two typical $FAPbI_3$ films with different PbI_2 contents under 400 nm excitation with a high fluence of 33 μJ cm^{-2}. Fig. 2a shows the 2D pseudo-color TA spectra of $FAPbI_3$-1 M with the lowest PbI_2 content. Except for a similar XB peak, the TA spectra under high excitation fluence exhibit a distinct feature compared to the low-fluence case. The TA spectrum at early delays exhibits a broad bleach signal extending into the high-energy region (to ~630 nm) due to the rapid evolution of initial nonequilibrium carriers into a Fermi–Dirac distribution.[42,43] As the delay time increases, this high-energy tail gradually narrows, which evolves over ~100 ps towards a symmetric XB peak centered at 783 nm (Fig. 2a), clearly reflecting the slowing down of the HC relaxation process. The significantly slowed down HC relaxation under high excitation intensity has already been widely observed in many perovskite films,[13,15] which is attributable to the remarkable HPB effect at high carrier densities. Fig. 2b presents the 2D pseudo-color TA image of $FAPbI_3$-1.5 M. Similarly, the TA spectra at early delays also show an obviously broadened bleach signal, indicating the presence of HPB in the sample. However, compared to $FAPbI_3$-1 M, $FAPbI_3$-1.5 M shows obviously narrower high-energy tails at initial delays (Fig. 2b and S5), suggesting the reduced HPB effect observed in the sample with excess PbI_2.

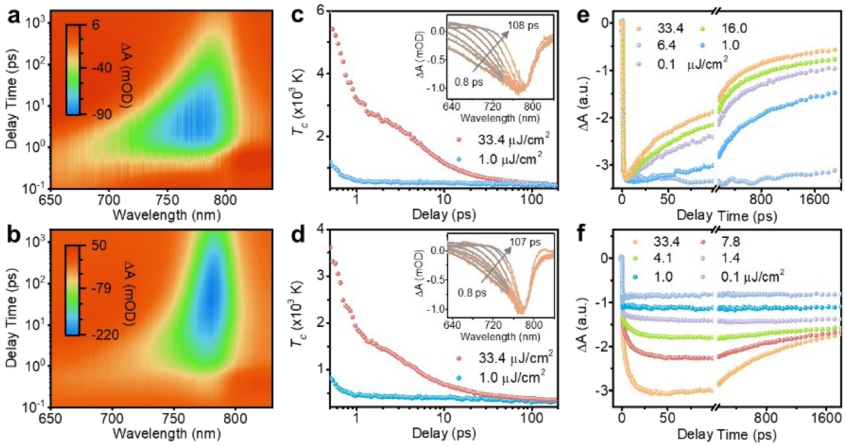

Fig. 2 Carrier dynamics of $FAPbI_3$-1 M and $FAPbI_3$-1.5 M. 2D pseudo-color images of TA spectra under 400 nm excitation at 33.4 μJ cm^{-2} for (a) $FAPbI_3$-1 M and (b) $FAPbI_3$-1.5 M. Temporal evolution of the carrier temperature T_c of (c) $FAPbI_3$-1 M and (d) $FAPbI_3$-1.5 M under 400 nm excitation at indicated excitation fluences. The insets show their fitted high energy tails at a higher fluence using the Maxwell–Boltzmann distribution function. Comparison of XB kinetics normalized at 1 ps delay of (e) $FAPbI_3$-1 M and (f) $FAPbI_3$-1.5 M under indicated excitation intensities.

In order to further compare the HPB effect, we extracted the carrier temperature (T_c) in the two samples by fitting the high-energy tail of TA spectra using a modified Maxwell–Boltzmann distribution (see the SI for a detailed description).[38] To ensure that HCs have reached a quasi-equilibrium temperature, the HC cooling kinetics was analyzed starting from 0.5 ps delay. Fig. 2c and d, respectively, compare the cooling curves of HCs in $FAPbI_3$-1 M and $FAPbI_3$-1.5 M under 400 nm excitation at two different excitation fluences. The insets show their TA spectral fitting at a high fluence, while those at a low fluence are shown in Fig. S6. At low excitation densities, HCs undergo rapid relaxation and T_c drops to room temperature within 1 ps, consistent with the ultrafast rise kinetics of the XB signal (see the insert in Fig. 1d), while under high excitation densities, the HCs exhibit a slower cooling rate, which even slows down to tens of ps, especially at later delays. Such slow HC cooling at high densities strongly confirms the presence of the HPB effect, which mainly originates from their large electron-phonon interaction, leading to the more rapid build-up of hot LO-phonon population and slower conversion rate from LO-phonons to acoustic phonons.[13,44] Compared with $FAPbI_3$-1 M, the initial T_c value of $FAPbI_3$-1.5 M is substantially lower, again confirming that the HPB effect is indeed reduced in the $FAPbI_3$-1.5 M film with a higher PbI_2 content, consistent with the observed narrower high-energy tail in the sample (Fig. 2b).

Compared with $FAPbI_3$-1 M, in addition to the reduced HPB effect, another more significant difference can be clearly observed in $FAPbI_3$-1.5 M, where its XB signal still shows a remarkable growth trend within a hundred ps at high excitation densities. To elucidate this strange behavior, we further examined the excitation-fluence dependence of XB kinetics in the two samples (Fig. 2e and f). Their pseudo-color TA maps under other excitation fluences are provided in Fig. S7 and S8. For the $FAPbI_3$-1 M film, although HC relaxation is remarkably slowed down at high excitation densities due to the HPB effect, its XB signal still reaches its maximum within a few ps due to the presence of stronger higher-order recombination, leading to its faster decay rate at higher densities. In stark contrast, for $FAPbI_3$-1.5 M, despite the weakened HPB effect, its XB signal rises very slowly and does not reach its maximum until ~100 ps under high excitation densities (Fig. 2f), suggesting a slow HC relaxation process. A similar slow-rising XB kinetic behavior has recently been observed in mixed-cation $FAPbI_3$ films and was attributed to the HC relaxation mediated by a polar cation induced intraband intermediate state.[16] However, unlike the above report, in which the slow-rising behavior also appeared at low excitation densities, our observation occurs specifically in $FAPbI_3$-1.5 M under high excitation fluences and is absent in $FAPbI_3$-1 M or at low fluences. This distinct dependence on the composition and excitation intensity suggests that the underlying HC relaxation mechanism in our system may differ subtly from the one previously reported.

Recent reports confirm that excess PbI_2 might create defect states higher than that of the CBM or VBM.[26,27] In order to confirm this, we conducted first-principles density functional theory (DFT) calculations to explore the electronic states of iodine vacancies (V_I) and interstitial iodine (I_I) in $FAPbI_3$ perovskite films. The results indicate that iodine-related defects introduce some localized electronic states above the CBM (Fig. S9), confirming the existence of intraband trap states (ITSs) induced by excess PbI_2. To explain the slow rising behavior of the XB signal in $FAPbI_3$-1.5 M, we presented a three-level kinetic model, in which the ITS above the lowest excited state (ES_1) is introduced to mediate HC relaxation (Fig. 3a). In $FAPbI_3$-1 M without ITSs, the photogenerated HCs relax directly to the ES_1 only *via* electron-phonon scattering, and thus no slow-rising XB kinetics is observed even at high densities. In contrast, in $FAPbI_3$-1.5 M with many ITSs, the photogenerated HCs may relax to the ES_1 through two different channels: (1) directly relaxing to the ES_1 *via* electron-phonon scattering at a rate of k_1; (2) first relaxing to the

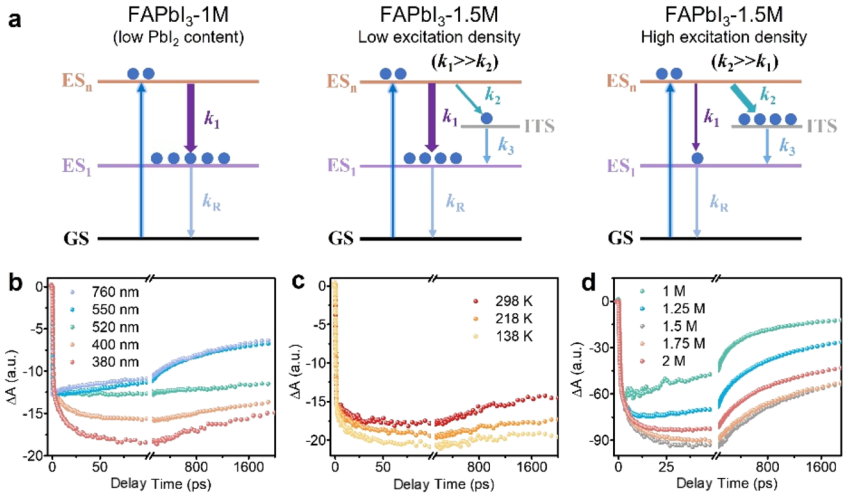

Fig. 3 Competition between direct and ITS-mediated HC relaxation pathways in $FAPbI_3$ films. (a) Schematic illustration of the HC relaxation process. ES, excited state; ITS, intraband trap state; GS, ground state. (b) XB kinetics of $FAPbI_3$-1.5 M under various excitation wavelengths with an initial carrier density of $\sim 3.3 \times 10^{18}$ cm^{-3}. (c) XB kinetics of $FAPbI_3$-1.5 M under 400 nm excitation at a high fluence of 33.4 μJ cm^{-2} at different temperatures. (d) XB kinetics of various $FAPbI_3$ films with different PbI_2 contents under 400 nm excitation at a fluence of 33.4 μJ cm^{-2}.

ITS at a rate of k_2 and then transferring from the ITS to the ES_1 at a relatively slow rate of k_3. At low excitation fluences, $k_1 >> k_2$, resulting in an inefficient ITS-mediated channel, and thus most carriers in $FAPbI_3$-1.5 M can directly relax rapidly to the ES_1, leading to the absence of a slow rising component, similar to the case of $FAPbI_3$-1 M. However, at high densities, the presence of a HPB can remarkably slow down the direct relaxation rate, resulting in $k_2 >> k_1$, which leads to most carriers first relaxing to the ITS and then transferring to the ES_1. Therefore, the slow-rising XB kinetics observed at high densities actually reflects the carrier transfer process from the ITS to the ES_1.

To verify the above mechanism, we next performed an excitation-wavelength-dependent TA measurement under relatively high excitation fluences (Fig. 3b). Note that, for comparability, the excitation fluence at different wavelengths was adjusted to ensure the same initial carrier density ($\sim 3.3 \times 10^{18}$ cm^{-3}) generated in the sample. As expected, the slow-rising XB kinetics is only observed under short-wavelength excitation, while it disappears when the excitation wavelength exceeds 520 nm. This indicates that photogenerated carriers require sufficient energy to populate into the ITS, confirming that the ITS level is higher than the ES_1. According to the excitation wavelength threshold, the ITS is estimated to be about 0.80 eV higher than the ES_1. To further understand the two relaxation channels, we conducted a temperature-dependent TA measurement under high excitation fluences (Fig. 3c). As the temperature decreases, both the rise time and amplitude of the slow component increase, suggesting a larger initial carrier population into the ITS. Since the HPB effect becomes more severe at lower temperatures due to less efficient phonon scattering,[14] the direct cooling channel will inevitably slow down, thereby enhancing the contribution from the ITS-mediated channel. These temperature-dependent results indicate that the slow-rising XB kinetics does stem from the ITS-mediated relaxation and can also be engineered by controlling the competition between the above two relaxation channels.

To further understand the role of excess PbI_2, we examined the HC relaxation kinetics in more $FAPbI_3$ films with different PbI_2 contents under high excitation densities (Fig. S10). The comparison of their XB kinetics is shown in Fig. 3d. For $FAPbI_3$-1 M with the lowest PbI_2 content, its XB kinetics does not show the slow-rising component after 1 ps, suggesting the negligible formation of ITSs likely due to insufficient PbI_2. With the increase of PbI_2 concentration from 1.25 M to 1.5 M, the amplitude of the slow-rising XB kinetics in these samples does remarkably increase, strongly confirming the formation of more ITSs. This results in more carriers populating into ITSs and thus less contribution from the direct relaxation channel, leading to a weaker HPB effect observed in the samples with higher PbI_2 contents (Fig. 2a, b and S10). We also note that, when the PbI_2 concentration exceeds 1.5 M, the amplitude of the slow-rising component shows a slight decrease, which might be related to the weakening of the HPB effect caused by material properties. Compared with $FAPbI_3$-1.5 M, the films containing more PbI_2 exhibit a smaller heat capacity (Fig. S11), which suggests faster heat conduction and a weaker HPB effect, leading to faster direct relaxation and less population into ITSs.

Slow cooling of HCs is highly desired for their effective extraction, but hard to realize because of the presence of strong electron-phonon interaction. Introducing an ITS *via* incorporating excess PbI_2 or other means might be an effective method to slow down the HC cooling and promote their extraction. To verify this idea, we fabricated three batches of $FAPbI_3$-1.5 M films *via* incorporating different electron acceptors, selected based on their band alignment with $FAPbI_3$ films (see the SI for detailed fabrication procedures).[45] Here, two kinds of SnO_2 were prepared *via* different methods (*i.e.*, commercial and ALD-deposited), resulting in slightly different bandgaps and are labeled as SnO_2(com.) and SnO_2(ALD), respectively. Fig. 4a–c show the band alignments of $FAPbI_3$ film and various acceptors, determined by ultraviolet photoelectron spectroscopy (Fig. S12 and S13). In principle, for ZnSe and SnO_2(com.), due to their

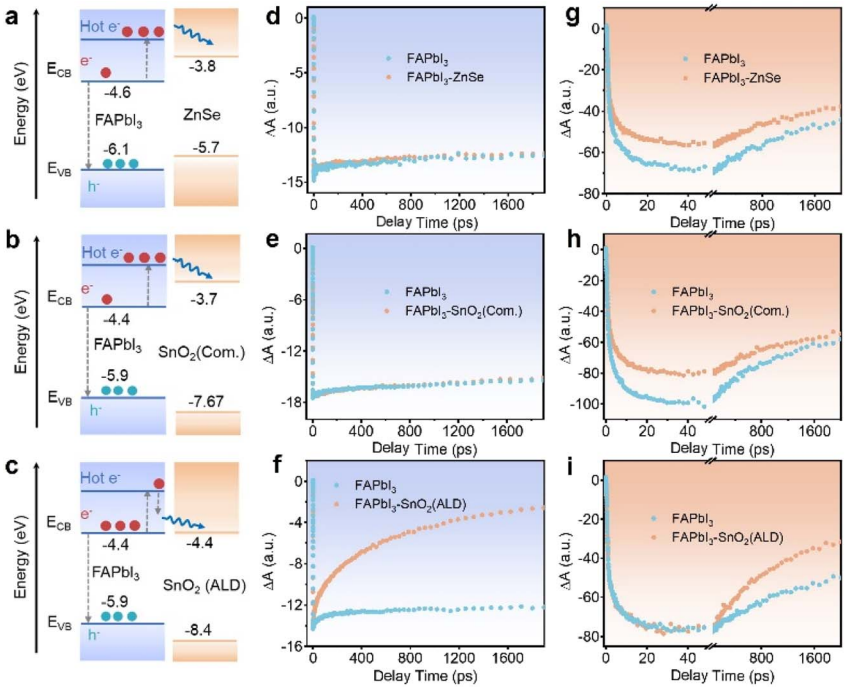

Fig. 4 Band alignment and HC extraction dynamics in $FAPbI_3$ films. (a–c) Energy level alignment of $FAPbI_3$-1.5 M interfaced with different electron acceptors: (a) ZnSe, (b) SnO_2(com.), and (c) SnO_2(ALD). (d–f) Comparison of XB kinetics in three sets of samples with and without (d) ZnSe, (e) SnO_2(com.) and (f) SnO_2(ALD) acceptors under near-bandgap excitation (760 nm, 2.7 μJ cm^{-2}). (g–i) Comparison of XB kinetics in three sets of samples with and without (g) ZnSe, (h) SnO_2(com.), and (i) SnO_2(ALD) acceptors under high-energy excitation (400 nm, 33.4 μJ cm^{-2}).

higher CBM levels than $FAPbI_3$, it is not possible to extract band-edge electrons, but it is possible to extract hot electrons, which is exactly opposite to SnO_2(ALD). Their abilities to extract band-edge carriers can also be directly reflected in the XB kinetic differences between the samples with and without acceptors under near-bandgap excitation at 760 nm (Fig. 4d–f). As expected, the dramatically faster recovery kinetics was observed in $FAPbI_3$-SnO_2(ALD) than in $FAPbI_3$, while for ZnSe and SnO_2(com.), no difference in their XB kinetics was observed between the samples with and without acceptors. On this basis, we further compared the XB kinetics in the samples with and without acceptors under 400 nm excitation at a high fluence of 33.4 μJ cm^{-2} (Fig. 4g–i). For the $FAPbI_3$-SnO_2(ALD) sample, no change was observed in the initial slow-rise kinetics (within 50 ps), suggesting that no hot electrons were extracted. In contrast, $FAPbI_3$-ZnSe and $FAPbI_3$-SnO_2(com.) exhibit a noticeable reduction in the amplitude of slow-rising component of XB kinetics, confirming that a fraction of hot electrons was successfully extracted into acceptors. These results strongly demonstrate the synergistic advantage of doping excess PbI_2 into perovskite films in conjunction with suitable electron acceptors, thereby retarding the HC relaxation and promoting their extraction. Based on this, we further fabricated two kinds of PSCs using $FAPbI_3$-1 M and $FAPbI_3$-1.5 M films and measured their *J–V* characteristics (Fig. S14). The results show that the PSC with a high PbI_2 content exhibits a higher PCE and a larger open-circuit voltage (V_{OC}) due to the excess energy of HC, demonstrating the positive influence of HC extraction on PCE.

Conclusions

In summary, we have investigated the influence of excess PbI_2 on the HC relaxation process in $FAPbI_3$ perovskite films by using femtosecond TA spectroscopy. The results show that excess PbI_2 in $FAPbI_3$ films significantly slows down the HC relaxation at high excitation densities by introducing an ITS-mediated channel, leading to the occurrence of a slow-rising component (extending to hundreds of ps) in their XB kinetics. Through engineering the competition between the direct relaxation and the ITS-mediated channel of HCs, this slow HC relaxation process can be controlled through adjusting the PbI_2 content, excitation density or temperature. Leveraging the prolonged HC lifetime, we successfully achieved the effective extraction of HCs in $FAPbI_3$ films containing excess PbI_2 by using an appropriate electron acceptor. Our findings suggest an effective method to slow down HC relaxation by creating ITSs, which might be beneficial for the development of next-generation HC devices.

Author contributions

W. T., J. L., Y. X. and S. J. conceived the project. X. Z. performed the sample preparation and characterization measurements. X. Z. conducted TA experiments with the assistance of X. T. X. Z. carried out the electron acceptor tests with the help of Q. S. and Q. D. Y. S. conducted DFT calculations. The manuscript was drafted by X. Z. and revised by J. L., Y. X., S. J. and W. T. All the authors discussed the results and contributed to the manuscript.

Conflicts of interest

There are no conflicts to declare.

Data availability

The data supporting this article have been included as part of the supplementary information (SI). Supplementary information: experimental details about sample preparation and TA measurements, additional TA data and other characterization results. See DOI: https://doi.org/10.1039/d6sc01780k.

Acknowledgements

This work was supported by the Strategic Priority Research Program of the Chinese Academy of Sciences (XDB0970302), the National Natural Science Foundation of China (22233005, 22439001, and 22171040), the CAS projects for Young Scientists in Basic Research (YSBR-007), the Natural Science Foundation of Liaoning (2024JH3/50100010), the Dalian Science and Technology Innovation Fund (2024RJ006), the DICP funding (DICP I202315) and the Shenyang Young and Middle-aged Science and Technology Innovation Talent Support Program, China (No. RC230784).

Notes and references

1 J. M. Ball and A. Petrozza, Defects in perovskite-halides and their effects in solar cells, *Nat. Energy*, 2016, **1**, 1–13.
2 M. Lee Michael, J. Teuscher, T. Miyasaka, T. N. Murakami and H. J. Snaith, Efficient Hybrid Solar Cells Based on Meso-Superstructured Organometal Halide Perovskites, *Science*, 2012, **338**, 643–647.
3 J.-P. Correa-Baena, M. Saliba, T. Buonassisi, M. Grätzel, A. Abate, W. Tress and A. Hagfeldt, Promises and challenges of perovskite solar cells, *Science*, 2017, **358**, 739–744.
4 A. J. Nozik, Utilizing hot electrons, *Nat. Energy*, 2018, **3**, 170–171.
5 A. P. Kirk and M. V. Fischetti, Fundamental limitations of hot-carrier solar cells, *Phys. Rev. B*, 2012, **86**, 165206.
6 J. Jeong, M. Kim, J. Seo, H. Lu, P. Ahlawat, A. Mishra, Y. Yang, M. A. Hope, F. T. Eickemeyer, M. Kim, Y. J. Yoon, I. W. Choi, B. P. Darwich, S. J. Choi, Y. Jo, J. H. Lee, B. Walker, S. M. Zakeeruddin, L. Emsley, U. Rothlisberger, A. Hagfeldt, D. S. Kim, M. Grätzel and J. Y. Kim, Pseudo-halide anion engineering for α-$FAPbI_3$ perovskite solar cells, *Nature*, 2021, **592**, 381–385.
7 J. Chen, M. E. Messing, K. Zheng and T. Pullerits, Cation-Dependent Hot Carrier Cooling in Halide Perovskite Nanocrystals, *J. Am. Chem. Soc.*, 2019, **141**, 3532–3540.
8 S. Sien Lim, D. Giovanni, Q. Zhang, A. Solanki, N. F. Jamaludin, J. W. Melvin Lim, N. Mathews, S. Mhaisalkar, M. S. Pshenichnikov and T. C. Sum, Hot carrier extraction in $CH_3NH_3PbI_3$ unveiled by pump-push-probe spectroscopy, *Sci. Adv.*, 2019, **5**, 3620.
9 J. Yin, R. Naphade, P. Maity, L. Gutiérrez-Arzaluz, D. Almalawi, I. S. Roqan, J.-L. Brédas, O. M. Bakr and O. F. Mohammed, Manipulation of hot carrier cooling dynamics in two-dimensional Dion-Jacobson hybrid perovskites via Rashba band splitting, *Nat. Commun.*, 2021, **12**, 3995.
10 P. Moazzezi, V. Yeddu, I. T. Cheong, M. R. Kokaba, S. Dayneko, Y. Ahmed and M. I. Saidaminov, Discovery of Perovskite Cosolvency and Undoped $FAPbI_3$ Single-Crystal Solar Cells Fabricated in Ambient Air, *J. Am. Chem. Soc.*, 2025, **147**, 10203–10211.
11 M. Geng, J. Li, K. Wang, L. Jiang, D. Lu, S. Iqbal, Y. Gu, L. Chen and T. Xu, Multiple functional bulk passivator pyrimidine derivative stabilizing perovskite precursors for efficient carbon-based perovskite solar cells, *Chem. Sci.*, 2025, **16**, 19317–19327.
12 H. Li, Q. Wang, Y. Oteki, C. Ding, D. Liu, Y. Guo, Y. Li, Y. Wei, D. Wang, Y. Yang, T. Masuda, M. Chen, Z. Zhang, T. Sogabe, S. Hayase, Y. Okada, S. Iikubo and Q. Shen, Enhanced Hot-Phonon Bottleneck Effect on Slowing Hot Carrier Cooling in Metal Halide Perovskite Quantum Dots with Alloyed A-Site, *Adv. Mater.*, 2023, **35**, 2301834.
13 Y. Yang, D. P. Ostrowski, R. M. France, K. Zhu, J. van de Lagemaat, J. M. Luther and M. C. Beard, Observation of a hot-phonon bottleneck in lead-iodide perovskites, *Nat. Photonics*, 2015, **10**, 53–59.
14 X. Yu, P. Shi, S. Gong, Y. Huang, J. Xue, R. Wang and X. Chen, Modulating hot carrier cooling and extraction with A-site organic cations in perovskites, *J. Chem. Phys.*, 2024, **160**, 121102.
15 J. Fu, Q. Xu, G. Han, B. Wu, C. H. A. Huan, M. L. Leek and T. C. Sum, Hot carrier cooling mechanisms in halide perovskites, *Nat. Commun.*, 2017, **8**, 1–9.
16 C. Wang, W. Chu, F. Ye, Z. Ou, Z. Li, Q. Guo, Z. Zheng, Z. Wang, X. Liu, G. Fang, O. Prezhdo, T. Wang and H. Xu, Polar methylammonium organic cations detune state coupling and extend hot-carrier lifetime in lead halide perovskites, *Chem*, 2022, **8**, 3051–3063.
17 B.-w. Park, N. Kedem, M. Kulbak, D. Y. Lee, W. S. Yang, N. J. Jeon, J. Seo, G. Kim, K. J. Kim, T. J. Shin, G. Hodes, D. Cahen and S. I. Seok, Understanding how excess lead iodide precursor improves halide perovskite solar cell performance, *Nat. Commun.*, 2018, **9**, 3301.
18 W. Shao, H. Wang, F. Ye, C. Wang, C. Wang, H. Cui, K. Dong, Y. Ge, T. Wang, W. Ke and G. Fang, Modulation of nucleation and crystallization in PbI_2 films promoting preferential perovskite orientation growth for efficient solar cells, *Energy Environ. Sci.*, 2023, **16**, 252–264.
19 D. Zhang, H. Zhang, H. Guo, F. Ye, S. Liu and Y. Wu, Stable α-$FAPbI_3$ in Inverted Perovskite Solar Cells with Efficiency Exceeding 22% via a Self-Passivation Strategy, *Adv. Funct. Mater.*, 2022, **32**, 2200174.
20 C. Luo, Y. Zhao, X. Wang, F. Gao and Q. Zhao, Self-Induced Type-I Band Alignment at Surface Grain Boundaries for Highly Efficient and Stable Perovskite Solar Cells, *Adv. Mater.*, 2021, **33**, 2103231.

21 Y. Gao, H. Raza, Z. Zhang, W. Chen and Z. Liu, Rethinking the Role of Excess/Residual Lead Iodide in Perovskite Solar Cells, *Adv. Funct. Mater.*, 2023, **33**, 2215171.

22 Z. Liu, P. Liu, M. Li, T. He, T. Liu, L. Yu and M. Yuan, Efficient and Stable FA-Rich Perovskite Photovoltaics: From Material Properties to Device Optimization, *Adv. Energy Mater.*, 2022, **12**, 2200111.

23 T. J. Jacobsson, J.-P. Correa-Baena, E. Halvani Anaraki, B. Philippe, S. D. Stranks, M. E. F. Bouduban, W. Tress, K. Schenk, J. Teuscher, J.-E. Moser, H. Rensmo and A. Hagfeldt, Unreacted PbI_2 as a Double-Edged Sword for Enhancing the Performance of Perovskite Solar Cells, *J. Am. Chem. Soc.*, 2016, **138**, 10331–10343.

24 Q. Jiang, Z. Chu, P. Wang, X. Yang, H. Liu, Y. Wang, Z. Yin, J. Wu, X. Zhang and J. You, Planar-Structure Perovskite Solar Cells with Efficiency beyond 21%, *Adv. Mater.*, 2017, **29**, 1703852.

25 S. Shin, P. Nandi, S. Seo, H. S. Jung, N. G. Park and H. Shin, Enhancing Stability of Efficient Perovskite Solar Cells (PCE $\approx$ 24.5%) by Suppressing PbI2 Inclusion Formation, *Adv. Funct. Mater.*, 2023, **33**, 2301213.

26 H. Chen, H. Yan and Y. Cai, Effects of Defect on Work Function and Energy Alignment of PbI_2: Implications for Solar Cell Applications, *Chem. Mater.*, 2022, **34**, 1020–1029.

27 F. Ren, H. Xiang, K. Zhao and C. Liu, Impacts of PbI_2 on high-efficiency perovskite solar cells: exploring intercalation orientations and defects, *J. Mater. Chem. C*, 2023, **11**, 13281–13289.

28 C.-J. Tong, L. Li, L.-M. Liu and O. V. Prezhdo, Long Carrier Lifetimes in PbI_2-Rich Perovskites Rationalized by Ab Initio Nonadiabatic Molecular Dynamics, *ACS Energy Lett.*, 2018, **3**, 1868–1874.

29 Y. Chen, Q. Meng, Y. Xiao, X. Zhang, J. Sun, C. B. Han, H. Gao, Y. Zhang, Y. Lu and H. Yan, Mechanism of PbI_2 in Situ Passivated Perovskite Films for Enhancing the Performance of Perovskite Solar Cells, *ACS Appl. Mater. Interfaces*, 2019, **11**, 44101–44108.

30 H. Y. Wang, M. Y. Hao, J. Han, M. Yu, Y. Qin, P. Zhang, Z. X. Guo, X. C. Ai and J. P. Zhang, Adverse Effects of Excess Residual PbI_2 on Photovoltaic Performance, Charge Separation, and Trap-State Properties in Mesoporous Structured Perovskite Solar Cells, *Chem. - Eur. J.*, 2017, **23**, 3986–3992.

31 A. D. Wright, C. Verdi, R. L. Milot, G. E. Eperon, M. A. Pérez-Osorio, H. J. Snaith, F. Giustino, M. B. Johnston and L. M. Herz, Electron-phonon coupling in hybrid lead halide perovskites, *Nat. Commun.*, 2016, **7**, 11755.

32 G. Kim, H. Min, K. S. Lee, D. Y. Lee, S. M. Yoon and S. I. Seok, Impact of strain relaxation on performance of α-formamidinium lead iodide perovskite solar cells, *science*, 2020, **370**, 108–112.

33 H. Min, M. Kim, S.-U. Lee, H. Kim, G. Kim, K. Choi, J. H. Lee and S. I. Seok, Efficient, stable solar cells by using inherent bandgap of a-phase formamidinium lead iodide, *science*, 2019, **366**, 749–753.

34 Z. Zheng, S. Wang, Y. Hu, Y. Rong, A. Mei and H. Han, Development of formamidinium lead iodide-based perovskite solar cells: efficiency and stability, *Chem. Sci.*, 2022, **13**, 2167–2183.

35 W. Hui, L. Chao, H. Lu, F. Xia, H. Wei, Z. Su, C. Niu, W. Tao, B. Du, D. Li, Y. Wang, H. Dong, S. Zuo, B. Li, W. Shi, X. Ran, P. Li, H. Zhang, Z. Wu, C. Ran, L. Song, G. Xing, X. Gao, J. Zhang, Y. Xia, Y. Chen and W. Huang, Stabilizing black-phase formamidinium perovskite formation at room temperature and high humidity, *Science*, 2021, **371**, 1359–1364.

36 S. Wang, Z. Miao, J. Yang, Z. Gu, P. Li, Y. Zhang and Y. Song, Lead-Chelating Intermediate for Air-Processed Phase-Pure FAPbI3 Perovskite Solar Cells, *Angew. Chem., Int. Ed.*, 2024, **63**, e202407192.

37 Y. Zhang, T. Yang, S.-U. Lee, S. Liu, K. Zhao and N.-G. Park, Stabilizing α-Phase $FAPbI_3$ Perovskite Induced by an Ordered Solvated Quasi-Crystalline PbI_2, *ACS Energy Lett.*, 2023, **9**, 159–167.

38 Y. Zhang, Y. Li, L. Zhang, H. Hu, Z. Tang, B. Xu and N. G. Park, Propylammonium Chloride Additive for Efficient and Stable $FAPbI_3$ Perovskite Solar Cells, *Adv. Energy Mater.*, 2021, **11**, 2102538.

39 T. Yan, C. Zhang, S. Li, Y. Wu, Q. Sun, Y. Cui and Y. Hao, Multifunctional Aminoglycoside Antibiotics Modified SnO_2 Enabling High Efficiency and Mechanical Stability Perovskite Solar Cells, *Adv. Funct. Mater.*, 2023, **33**, 2302336.

40 J. Yang, X. Wen, H. Xia, R. Sheng, Q. Ma, J. Kim, P. Tapping, T. Harada, T. W. Kee, F. Huang, Y.-B. Cheng, M. Green, A. Ho-Baillie, S. Huang, S. Shrestha, R. Patterson and G. Conibeer, Acoustic-optical phonon up-conversion and hot-phonon bottleneck in lead-halide perovskites, *Nat. Commun.*, 2017, **8**, 14120.

41 S. Wang, J. Leng, Y. Yin, J. Liu, K. Wu and S. Jin, Ultrafast Dopant-Induced Exciton Auger-like Recombination in Mn-Doped Perovskite Nanocrystals, *ACS Energy Lett.*, 2020, **5**, 328–334.

42 R. Zhang, Z. Zhou, X. Li, T. Pang, T. Song, H. Wu, Q. Liao, Z. Wang, F. Huang, K. Wu and D. Chen, Low-Threshold and Ultrastable Amplified Spontaneous Emission from $CsPbBr_3$@Glass via Glass Network Modulation, *ACS Nano*, 2025, **19**, 14318–14329.

43 S. Zheng, Q. Huang, W. Niu, R. Chen, T. Pang, L. Zeng and D. Chen, Tailoring Carrier Dynamics by Band Alignment Engineering in Quasi-2D Perovskite LED, *Nano Lett.*, 2025, **25**, 15927–15936.

44 M. B. Price, J. Butkus, T. C. Jellicoe, A. Sadhanala, A. Briane, J. E. Halpert, K. Broch, J. M. Hodgkiss, R. H. Friend and F. Deschler, Hot-carrier cooling and photoinduced refractive index changes in organic–inorganic lead halide perovskites, *Nat. Commun.*, 2015, **6**, 8420.

45 Y. Chen, Y. Lei, Y. Li, Y. Yu, J. Cai, M.-H. Chiu, R. Rao, Y. Gu, C. Wang, W. Choi, H. Hu, C. Wang, Y. Li, J. Song, J. Zhang, B. Qi, M. Lin, Z. Zhang, A. E. Islam, B. Maruyama, S. Dayeh, L.-J. Li, K. Yang, Y.-H. Lo and S. Xu, Strain engineering and epitaxial stabilization of halide perovskites, *Nature*, 2020, **577**, 209–215.